Capacitance Splines for Arbitrary Doping Variations

31th BipAK Workshop, Nov. 08th and 9th, 2018 AdMOS, Frickenhausen, Germany

Letter Session

Zoltan Huszka, amsAG and Michael Schröter, TUD

Capacitance Splines for Arbitrary Doping Variations

1. The standard capacitance-charge functions

The *standard* functions describing the electrostatics around a *p-n* junction read

$$\text{junction capacitance: } C_j = C_{j0}\left(1-\frac{V_j}{V_D}\right)^{-z} \tag{1}$$

$$\text{stored electrostatic charge } Q_j = C_{j0}\frac{V_D}{1-z}\left[1-\left(1-\frac{V_j}{V_D}\right)^{1-z}\right] \tag{2}$$

For removing the pole from (1) the standard Gummel-Poon model (SGPM) adopts a linear exension to the capacitance from a selected forward knee voltage

$$V_f = fc \cdot V_D \tag{3}$$

Whereas $fc < 1$ is a scalar model parameter in SGPM it is defined in Hicum (for the CB junction) as

$$fc = 1 - 2.4^{(-1/z)} \tag{4}$$

For sparing the computation of the expensive power function (4) will be approximated by a fifth order polynomial

$$\text{fc} = 0.995 * (0.9948 + \text{zci} * (0.2304 + \text{zci} * (-1.4668 + \text{zci} * (-0.0122 + \text{zci} * (1.9279 + \text{zci} * (-1.0946)))))) \tag{5}$$

The cofactor `0.995` avoids $fc \geq 1$ occuring at the approximation for small grading coefficients.

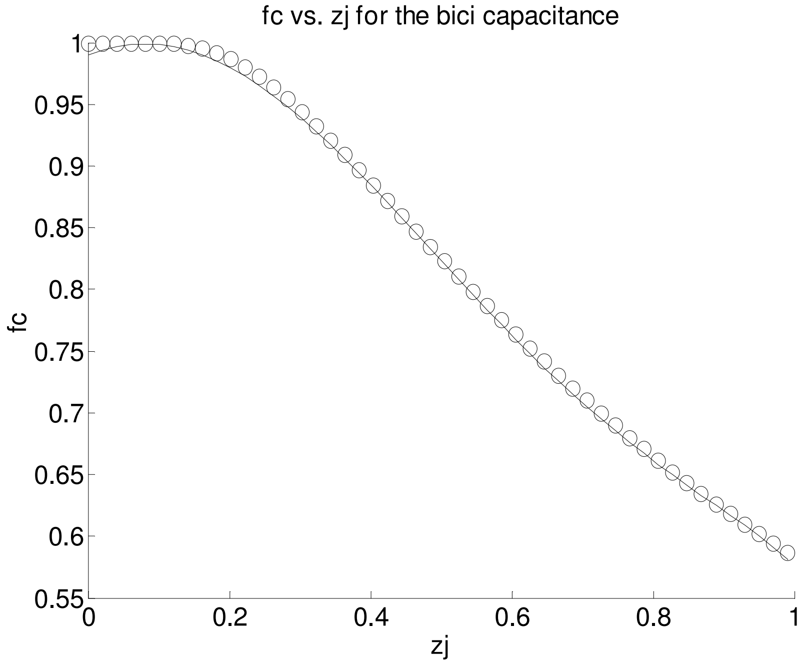

Fig. 1 Approximation of `fc`, symbols: eq. (4), line: eq. (5)

Using (4) and (5) one can derive with

$$pwq = (1-fc)^{-z-1} \tag{6}$$

the full standad capacitance and charge formulas

$$C_j(V_j)=\begin{cases} V_j \geq V_f & C_{j0}pwq\left(1-fc+z\dfrac{V_j-V_f}{V_D}\right) \\ V_j < V_f & C_{j0}\left(1-\dfrac{V_j}{V_D}\right)^{-z} \end{cases} \tag{7}$$

$$Q_j(V_j)=\begin{cases} V_j \geq V_f & C_{j0}\dfrac{V_D}{1-z}\left[1-(1-fc)^2\,pwq\right]+C_{j0}pwq(V_j-V_f)\left[(1-fc)+z\dfrac{V_j-V_f}{2V_D}\right] \\ V_j < V_f & C_{j0}\dfrac{V_D}{1-z}\left[1-\left(1-\dfrac{V_j}{V_D}\right)^{1-z}\right] \end{cases} \tag{8}$$

2. Generalized capacitance functions

The total voltage across an *n-p* junction is described by

$$V_{tot}=\frac{1}{\varepsilon\varepsilon_0}\int_{-d_n}^{d_p} x\cdot\sigma(x)dx$$

with $\sigma(x)$ as the space charge. For simplicity a one sided *n-p* junction is regarded with $d_n=0$ and $d_p=W$ yielding

$$V_{tot}=\frac{1}{\varepsilon\varepsilon_0}\int_{0}^{W} x\cdot\sigma(x)dx \tag{9}$$

The voltage gradient of the junction capacitance $C_j(V_{tot})=\dfrac{\varepsilon\varepsilon_0}{W}$ over unit area becomes with $\sigma=-qN_A$

$$\frac{\partial C_j}{\partial V_{tot}}=-\frac{\varepsilon\varepsilon_0}{W^2}\frac{\partial W}{\partial V_{tot}}=\frac{(\varepsilon\varepsilon_0)^2}{q}\frac{1}{W^3\cdot N_A(W)} \tag{10}$$

It is always positive. The second derivative results in

$$\frac{\partial^2 C_j}{\partial V_{tot}^2}=\frac{(\varepsilon\varepsilon_0)^3}{q^2\cdot W^4\cdot N_A^2(W)}\left[\frac{3}{W}+\frac{d\left[\ln(N_A(W))\right]}{dW}\right] \tag{11}$$

The approximations will be categorized according to the behaviour of the derivatives.

- 2.1 *Punch through type capacitance*

The capacitance gradient (10) is uniformly proportional to C_j^3 at constant or slightly varying $N_A(W)$. A strongly increasing doping concentration implies an additional flattening which can not be described by a single-piece classical model any more.
The second derivative (11) remains all along positive like that of (1). This property is preserved by a capacitance function composed of standard segments contacting each other in value and derivative at selected voltage points. The sections will be spanned between the voltage knot points

$$V_{K,N}<\cdots V_{K,n}<\cdots V_{K,2}<V_{K,1} \tag{12}$$

The first knot can be any number satisfying

$$V_{K,1}<V_f \tag{13}$$

The capacitance of the zero indexed knot is written as (1)

$$C_j=C_{j0}\left(1-\frac{V_j}{V_D}\right)^{-z} \tag{14}$$

and referred to as the primary branch.
The capacitance piece *n*

$$C_{j,n} = C_{j0,n}\left(1-\frac{V_j - V_{K,n}}{V_{D,n}}\right)^{-z_n} \tag{15}$$

is valid in the bias interval

$$V_{K,n+1} \le V_j \le V_{K,n}; \quad n > 0 \tag{16}$$

Continuity of the values in $V_j = V_{K,n+1}$ defines the relation between the zero bias capacitances

$$C_{j0,n+1} = C_{j0,n}\left(1-\frac{V_{K,n+1} - V_{K,n}}{V_{D,n}}\right)^{-z_n} \tag{17}$$

Derivatives in the knots read:

$$\begin{aligned} \dot{C}_{j,n}(V_{K,n+1}) &= C_{j0,n+1}\frac{z_n}{V_{D,n}}\frac{1}{1-\dfrac{V_{K,n+1}-V_{K,n}}{V_{D,n}}} \\ \dot{C}_{j,n+1}(V_{K,n+1}) &= C_{j0,n+1}\frac{z_{n+1}}{V_{D,n+1}} \end{aligned} \tag{18}$$

The continuity of the first derivatives in $V_{K,n+1}$ requires

$$V_{D,n+1} = V_{D,n}\frac{z_{n+1}}{z_n}\left[1-\frac{V_{K,n+1}-V_{K,n}}{V_{D,n}}\right] \tag{19}$$

Index $n = 0$ refers to the primary function (14) with $V_{K,0} = 0$ and omitted zero indices.
The charge expresion in the *n*-th section is

$$Q_{j,n} = C_{j0,n}\cdot\frac{V_{D,n}}{1-z_n}\left[1-\left(1-\frac{V_j - V_{K,n}}{V_{D,n}}\right)^{1-z_n}\right] \tag{20}$$

The charge is incremented in the *n-th* zone by

$$Q_{j,n}^{incr} = C_{j0,n}\cdot\frac{V_{D,n}}{1-z_n}\left[1-\left(1-\frac{V_{K,n+1} - V_{K,n}}{V_{D,n}}\right)^{1-z_n}\right] \tag{21}$$

The actual charge in the *n-th* section results in

$$Q_{j,n}(V_j) = Q_{j,n-1}^{tot} + C_{j0,n}\cdot\frac{V_{D,n}}{1-z_n}\left[1-\left(1-\frac{V_j - V_{K,n}}{V_{D,n}}\right)^{1-z_n}\right] \tag{22}$$

with

$$Q_{j,n-1}^{tot} = Q_{j,n-2}^{incr} + Q_{j,n-3}^{incr} + \cdots + Q_{j,0}^{tot} \tag{23}$$

- 2.2 ***Inflexion type capacitance***

A sign change of the square bracketed term in the second derivative (11) identifies an inflexion point in the capacitance curve. For hyperabrupt doping densities the inflexion can be visible even before punch-through or breakdown masked it. As a further example assume a doping function of the type

$$N = N_0 + N_p \exp\left[-\left(\frac{W - W_p}{W_0}\right)^2\right] \tag{24}$$

When $N_p >> N_0$ the second term is dominating around the peak position W_p. With this condition the root of (11) that is, the position of the inflexion yields

$$W_{\text{infl}} = \frac{W_p + \sqrt{W_p^2 + 6W_0^2}}{2} \tag{25}$$

As expected the inflexion occurs at the falling part of the doping function. (24) is a reasonable approximation of a doping spike occasionally introduced in the collector of III-V HBTs for performance improvements. The linearity of bipolar amplifiers characterized by the preferably large third order intercept OIP3 ultimately depends on the nonlinearity of the collector capacitance. The OIP3 can be maximized by linearizing C_{BC} as much as possible [1]. The linearity condition is well satisfied in the neighbourhood of the inflexion point $\frac{\partial^2 C_{BC}}{\partial V_{BC}^2} = 0$.
Note that (25) makes it possible to estimate the position of the linearization spike from the inflexion point capacitance.
A mixed capacitance spline will be composed of cubic segments sandwiched between standard arcs (1). The cubic positions are selected so as to overlap the inflexion intervals of the measured capacitance curve. There may be more than one inflexion which case every such interval shall be covered by separate cubics between standard capacitances. The leading and trailing curve sections are always standard capacitance functions.
The discussion is restricted to the single inflexion case. The procedure can be easily extended to the unlikely situation when the measurements reflect two or more inflexions.
A pair of left and right bias points $V_{jL} < V_{jR}$ are selected around the ends of the inflexion zone. Using the capacitance values C_{j0L}, C_{j0R} in these locations the trailing and leading curves with their derivatives read

$$C_{jL} = C_{j0L}\left(1 - \frac{V_j - V_{jL}}{V_{DL}}\right)^{-z_L} \quad V_j \le V_{jL} \qquad \dot{C}_{jL} = \frac{z_L C_{j0L}}{V_{DL}} \quad V_j = V_{jL} \tag{26}$$

and

$$C_{jR} = C_{j0R}\left(1 - \frac{V_j - V_{jR}}{VD}\right)^{-z_R} \quad V_j \ge V_{jR} \qquad \dot{C}_{jR} = \frac{z_R C_{j0R}}{VD} \quad V_j = V_{jR} \tag{27}$$

where

$$VD = V_{DR} - V_{jR} \tag{28}$$

The leading curve at $V_j \ge V_f$ is linearly extended as shown by (7), (8). The forward knee point is now

$$V_f = V_{jR} + fc \cdot VD \tag{29}$$

With the variable transformation

$$u = V_j - V_{jR} \tag{30}$$

the cubic with the width of the interval

$$V_{RL} = V_{jR} - V_{jL} \tag{31}$$

is constructed as

$$\begin{gathered} -V_{RL} \le u \le 0 \\ p_3(u) = a_3 u^3 + a_2 u^2 + a_1 u + a_0 \end{gathered} \tag{32}$$

Observing the boundary conditions the coefficients read

$$
\begin{aligned}
a_0 &= C_{j0R} \\
a_1 &= \dot{C}_{j0R} \\
a_2 &= \frac{u_{RL}(\dot{C}_{j0L} + 2\dot{C}_{j0R}) - 3(C_{j0R} - C_{j0L})}{u_{RL}^2} \\
a_3 &= \frac{u_{RL}(\dot{C}_{j0L} + \dot{C}_{j0R}) - 2(C_{j0R} - C_{j0L})}{u_{RL}^3}
\end{aligned}
\tag{33}
$$

The integration for the regional charges will be started from the point $V_j = V_{jR}$ implying $Q_j^{(R)}(V_{jR}) = 0$. This is corrected by the residue $Q_{jz} = Q_j^{(R)}(0)$ computed in the interval including $V_j = 0$ to obtain charge conservation

$$
Q_j = Q_j^{(R)}(V_j) - Q_{jz} \tag{34}
$$

Leading branch:
$V_{jR} \le V_j < V_f$

$$
Q_j^{(R)} = C_{j0R} \frac{VD}{1 - z_R} \left[1 - \left(1 - \frac{V_j - V_{jR}}{VD} \right)^{1 - z_R} \right] \tag{35}
$$

Linear extension:
$V_j \ge V_f$

$$
\begin{aligned}
&pwq = (1 - fc)^{-z_R - 1} \\
&Q_j^{(R)} == C_{j0R} \frac{VD}{1 - z_R} \left[1 - (1 - fc)^2 \, pwq \right] + C_{j0R} \, pwq (V_j - V_f) \left[(1 - fc) + z_R \frac{V_j - V_f}{2VD} \right]
\end{aligned}
\tag{36}
$$

Cubic link
$V_{jL} < V_j < V_{jR}$
the charge in the third order link reads

$$
\begin{aligned}
&-V_{RL} \le u \le V_j - V_{jR} \\
&Q_j^{(R)}(u) = u \left(a_0 + u \left(\frac{a_1}{2} + u \left(\frac{a_2}{3} + u \frac{a_3}{4} \right) \right) \right)
\end{aligned}
\tag{37}
$$

Trailing branch
$V_j < V_{jL}$
The charge incremented by the cubic region

$$
Q_{j3} = -V_{RL} \left(a_0 - V_{RL} \left(\frac{a_1}{2} - V_{RL} \left(\frac{a_2}{3} - V_{RL} \frac{a_3}{4} \right) \right) \right) \tag{38}
$$

implies

$$
Q_j^{(R)} = Q_{j3} + C_{j0L} \frac{V_{DL}}{1 - z_L} \left[1 - \left(1 - \frac{V_j - V_{jL}}{V_{DL}} \right)^{1 - z_L} \right] \tag{39}
$$

3. Verification

All tests were made in Verilog-A using QucsStudio_v2.4.1. The capacitances were obtained from the charge by the `ddx()` system function.

- 3.1 *Punch through model*

A capacitance spline of two sections will be considered. There is one knot point

$$V_{K,1} = -vpt \tag{40}$$

with vpt as a model parameter. A standard capacitance function is linked in the first order to the primary forward branch at $V_j = -vpti$ selecting

$$vpti = kvpt(vpt - V_D) \tag{41}$$

In (41) $kvpt = 0.8$ is a constant empirical factor for providing the best fit to the Hicum punch through model QJMOD [2]. With a further empirical constant

$$hz = 0.22 \tag{42}$$

and introducing

$$z_p = hz \cdot z \tag{43}$$

$$V_{Dp} = hz \cdot (V_D + vpt) \tag{44}$$

$$V_{jp} = V_j + vpti \tag{45}$$

we have the knot point quantities

$$\gamma_{jp} = \left(1 + \frac{vpti}{V_D}\right)^{-z} \tag{46}$$

$$Q_{j0}^{tot} = C_{j0} \frac{V_D}{1-z} \left[1 - \left(1 + \frac{vpti}{V_D}\right) \cdot \gamma_{jp}\right] \tag{47}$$

Now the charge within the punch-through section yields as

$$Q_{jp} = C_{j0} \gamma_{jp} \frac{V_{Dp}}{1 - z_p} \left[1 - \left(1 - \frac{V_{jp}}{V_{Dp}}\right)^{1-z_p}\right] \tag{48}$$

providing the regional charge function

$$Q_j(V_j) = \begin{cases} V_j \ge V_f & C_{j0} \frac{V_D}{1-z}\left[1 - (1-fc)^2 pwq\right] + C_{j0} pwq (V_j - V_f)\left[(1-fc) + z\frac{V_j - V_f}{2V_D}\right] \\ -vpti \le V_j < V_f & C_{j0} \frac{V_D}{1-z}\left[1 - \left(1 - \frac{V_j}{V_D}\right)^{1-z}\right] \\ V_j < -vpti & Q_{jp} + Q_{j0}^{tot} \end{cases} \tag{49}$$

Parameter fc is computed by (5). The capacitance is automatically generated by derivation in Verilog-A.

Fig. 2 and Fig. 3 demostrate a comparision of the spline concept to the Hicum model described by the Manual [2] and the QJMOD macro in the released Verilog-A codes. The tests were made with 4 parameter sets shown in Table 1.

Table 1.
parameter sets

	zci	vdci	cjci0
1	0.16	0.20	1
2	0.33	0.75	1
3	0.67	0.40	1
4	0.90	0.55	1

For a better visibility the small
vpt=1V ,2V, 5V
and large
vpt=10V, 20V, 50V
groups are shown on plots of different Vbias axis scaling. The proposed capacitance spline approach provides equivalent results with the existing punch-through model.

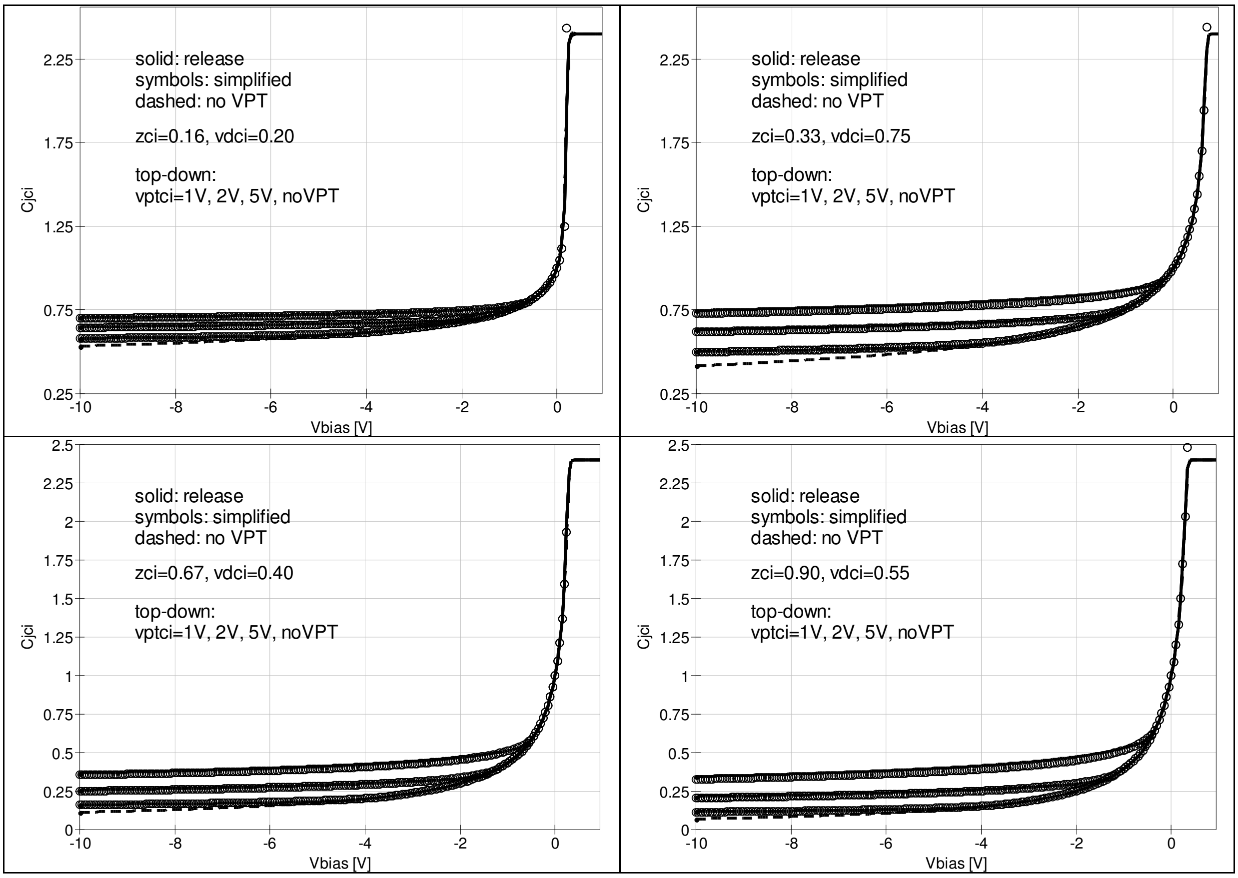

Fig. 2 The small vpt group

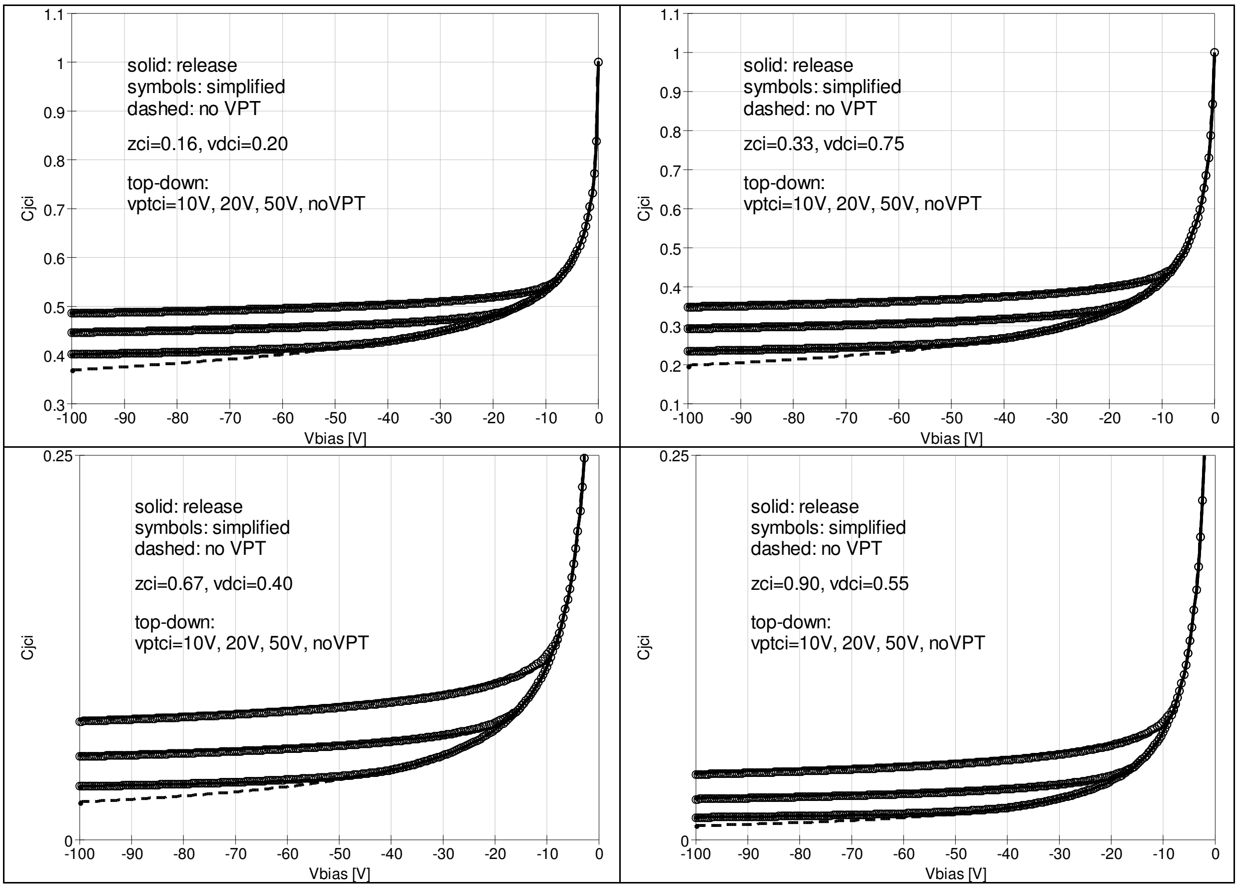

Fig. 3 The large vpt group

- 3.2 *Inflexion type capacitance*

A mixed capacitance spline consisting of two standard arcs linked by a cubic polynomial is used. Equations (26)...(39) have been adopted for the model.
In lack of direct data the InP measurement points on the plot found in [3] have been digitized. Both [4] and the mixed cubic model proposed here were fit to this data.

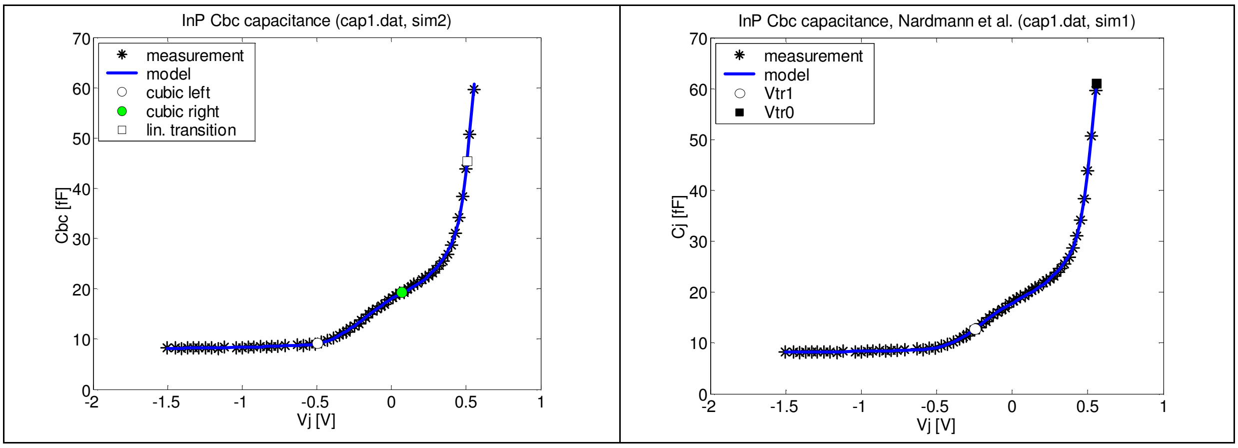

Fig. 4 Modeling an InP [3] capacitance by mixed cubic splines (left) and by method [4] (right)

Fig. 4 demostrates the same modeling quality for the two approaches. The marks indicate the cardinal points of the two concepts. Observe the linearity of the curve in the inflexion region.

4. Simulation speed

The simulation times were obtained from QucsStudio_v2.4.1 using a dedicated Verilog-A code including only the capacitance models. The charge computations were repetitively performed by the number indicated in the plot titles. Notations:

```
QJMOD       punch-through charge model of Hicum [2], exp-log transitions
QJMODF      charge model of Hicum [2] w/o punch-through, hyp. transition
CAPSPL      capacitance spline model of Chapter 2.1, linear extension
NARDMANN    model of [4], exp-log transitions
MIXSPL      mixed cubic splines of Chapter 2.2, linear extension
SGPM        standard model, linear extension
```

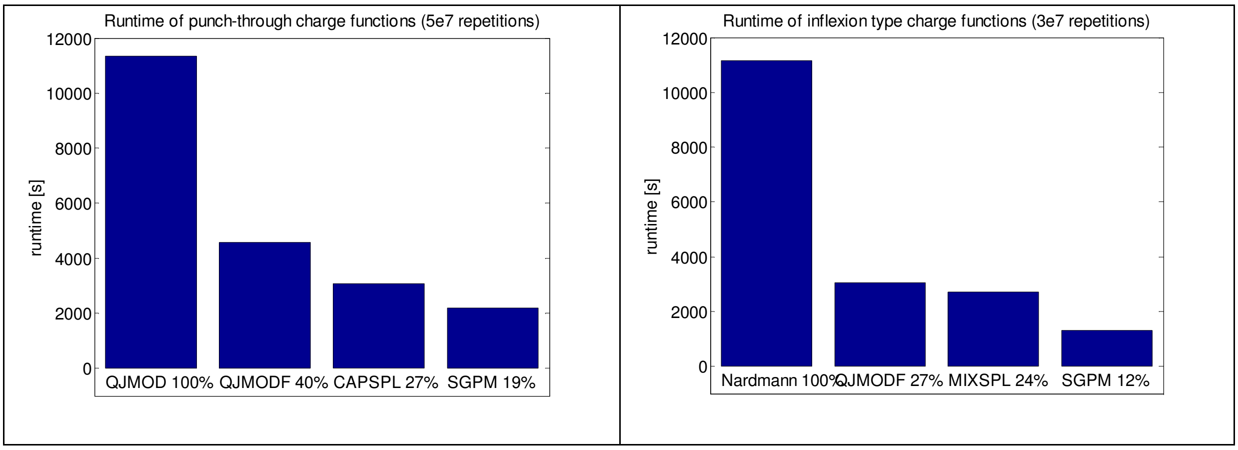

Fig. Comparision of the simulation times of the different models: punch-through (left), inflexion (right). Ratios to the slowest model shown in %.

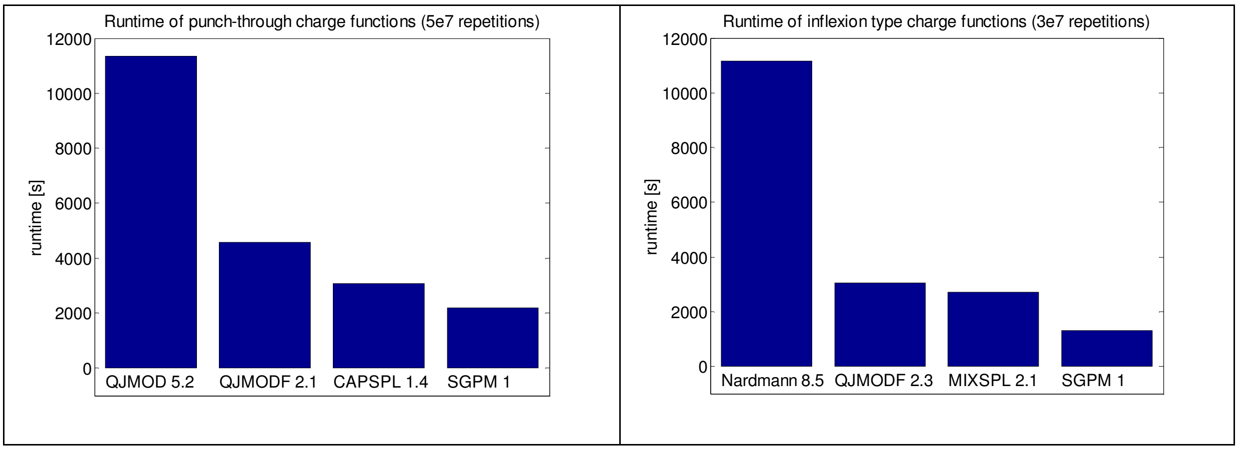

Fig. Comparision of the simulation times of the different models: punch-through (left), inflexion (right). Ratios to SGPM shown on the x-axis labels.

Summary

- a pure capacitance spline has been proposed to model the punch-through type capacitances
- a mixed capacitance-cubic spline was constructed to account for the inflexion type capacitance functions
- the two approaches can be combined if measurements require
- both variants provided results of equivalent quality to the former solutions
- the proposed updates run approximately 4-times faster than the existing codes
- the new punch-through approach takes a factor of 1.4 larger runtime than the SGPM. As seen from (49) only the $V_j < -vpti$ region needs two expensive power function evaluations, the other two can be solved by one such operation like the standard.
- out of the four regions of the inflexion charge, three zones require two power function evaluations while the remaining cubic section can be solved only by Q_{jz}. That is why the effort is about twice of the SGPM computation.
- as a conclusion, the runtimes of the new (vs. the former) vpt and inflexion approaches to SGPM increase by 1.4 (vs. 5.2) and by 2.1 (vs. 8.5) times respectively
- besides these improvements the proposed solutions preserve the standard capacitance sections as they are without distortions imposed by transition functions

References

[1] J.M.M. van der Meulen and L.C.N. de Vreede, „Enhanced Bipolar Transistor Design for the Linearization of the Base-Collector Capacitance," Bipolar/BiCMOS Circuits and Technology Meeting, 2017, pp. 126-129.

[2] M. Schroter, A. Pawlak, A. Mukherjee, „HICUM / L2, A geometry scalable physics-based compact bipolar transistor model", August, 2015. Available: https://www.iee.et.tu-dresden.de/iee/eb/hic_new/hic_doc.html#hicumL2

[3] A. Pawlak, „Regional approach," private communication

[4] Tobias Nardmann, Michael Schroter and Paulius Sakalas, „A Multiregion Approach to Modeling the Base-Collector Junction Capacitance," IEEE Trans. on El. Dev. VOL.63, NO9, SEPTEMBER 2016

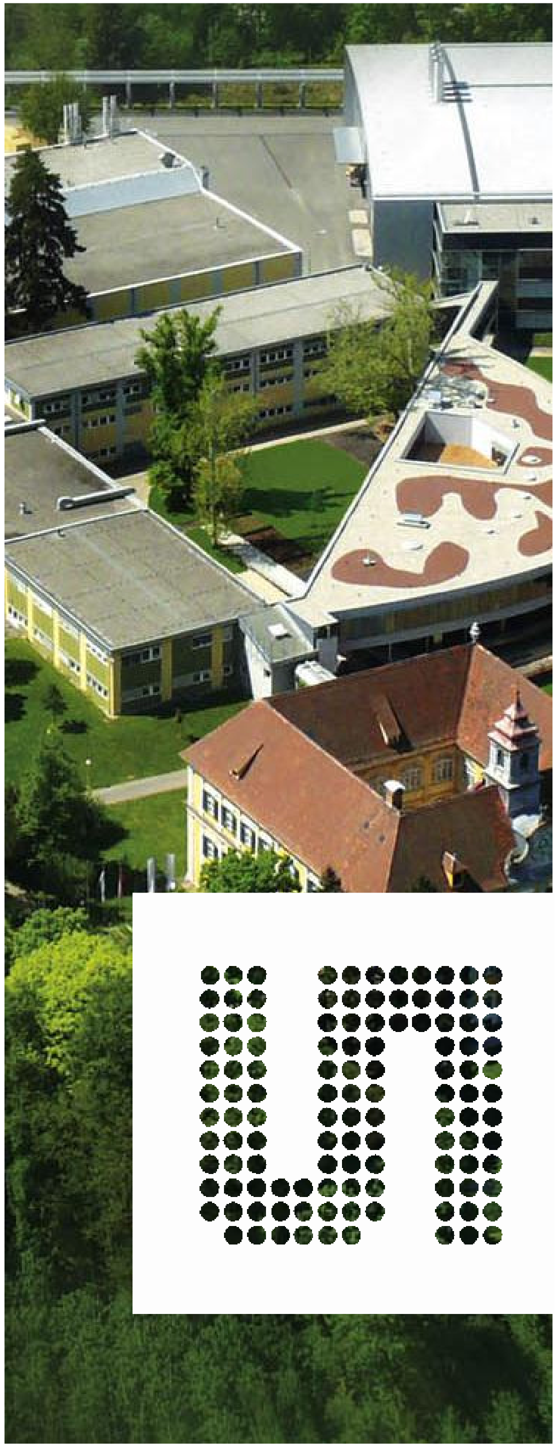

Thank for your attention!

Please visit our website www.ams.com